

Performance and use of composite-substrate-based bipolar lead/acid batteries for pulsed-power applications

Michel Saakes^{a,*}, Dion Schellevis^a, Dieter van Trier^a, Maurice Wollersheim^b

^a TNO-Environment, Energy and Process Innovation, PO Box 6011, 2600 JA Delft, The Netherlands

^b TNO PML-Pulse Physics Laboratory, PO Box 45, 2280 AA Rijswijk, The Netherlands

Received 7 August 1996; accepted 16 November 1996

Abstract

A new type of composite substrate is proposed for constructing fast discharge bipolar lead/acid batteries. This newly developed substrate, used for constructing 4 V bipolar lead/acid batteries, displays no corrosion and a very low catalytic effect for both hydrogen and oxygen evolution. The specific resistance is $1.2 \Omega \text{ cm}$ while the areal resistance is $0.04 \Omega \text{ cm}^2$. The active layers are formed by the Planté formation method, both in situ and ex situ. For pulsed-power applications, where energy is quickly transferred to an inductor, a model calculation is given for deriving the required ratio of the specific power and the specific energy. © 1997 Published by Elsevier Science S.A.

Keywords: Lead/acid batteries; Pulsed-power applications; Composite substrates

1. Introduction

During the last decade, the development of lead/acid batteries has undergone much progress. Examples of this development are valve-regulated recombinant lead/acid batteries (maintenance-free) [1], a thin-film battery developed by Bolder Technologies [2], and a bipolar lead/acid battery developed by Johnson Controls [3], Arias Research Associates [4–6], and Bipolar Technology [7–9]. These advances represent a major step forward both in traditional and possible new areas of application of lead/acid batteries. Especially, the need for (hybrid) electric vehicles gives a great impetus to the development of these types of lead/acid battery. One possible application for lead/acid batteries is powering electric armament (e.g., pulsed lasers, high power microwaves, electric energy guns) [10,11]. Because of the very large current pulses (several hundreds of kA for tens of ms) involved at a relative high voltage (several hundreds of volt), the use of conventional lead/acid batteries (e.g., automotive batteries) would lead to an unacceptable high weight for the battery package

because of the relatively low specific power of current batteries (limited at approximately 200 W kg^{-1}). Only a significant increase in specific power would bring a pulsed-power application within reach. One way to achieve this is to use a bipolar battery configuration as has been demonstrated at the Pulse Physics Laboratory [10–13]. It has been shown that, in principle, a specific power of 1 kW kg^{-1} or more with lead plates is feasible with a fast discharge bipolar lead/acid battery [3,11].

The development of such bipolar lead/acid batteries has been delayed, however, as a good candidate for the bipolar plate is still missing. The material for the bipolar plate must fulfill the following requirements: low density; chemically stable in sulfuric acid; electrochemically stable towards lead dioxide (no corrosion); good conductivity; no catalytic effects on the evolution of hydrogen and oxygen gas; mechanical and dimensional stability; flexibility; low cost, and non-toxicity.

Pure lead is subject to corrosion when used as a substrate for the bipolar plate. Especially, the presence of lead dioxide and sulfuric acid places extreme demands on the electrochemical and chemical stability of the substrate material which is covered on one side with lead dioxide and on the other side with lead. Many materials have been proposed in literature and patents to serve as a substrate. Among these materials, lead alloys are often used.

* Corresponding author.

Non-metallic substrates are commonly composed by a thermoplastic (e.g., polyethylene (PE), polypropylene (PP)) and carbon black or Ketjen black (AKZO, The Netherlands) [14]. The use of PE or PP composite substrate for bipolar plates is limited, however, to systems with lower standard potential than the $\text{PbO}_2/\text{PbSO}_4$ couple present in sulfuric acid [15]. The lead–boron tetrafluoride battery can, due to its lower standard potential, be made bipolar using a substrate of PP filled with graphite for the bipolar plate.

The use of polyolefine thermoplastics filled with an electrical conductor can be extended to systems with extreme high standard potentials, such as $\text{PbO}_2/\text{PbSO}_4$, if the positive side of the substrate is protected with, for example, SnO_2 [8]. Also, a coating of barium metaplumbate (BaPbO_3) is used to protect the substrate from oxidation [16]. An important disadvantage of thermoplastics filled with graphite is the dimensional stability. A way to overcome this problem is to use a matrix of glass fibres [17]. These fibres are covered with SnO_2 , doped with F [18], for obtaining a good conductivity.

The substrate can also be made of metals other than lead, e.g., titanium or iron. In the case of titanium [19], a protective layer is used and contains an epoxy resin with a dispersion of conductive filler selected from graphite or lead. With iron [20], a coating of nickel has been used, covered on the positive side with SnO_2 and on the negative side with lead.

The present study employs a new type of substrate, which can be described as a composite substrate. The aim is to combine a number of advantages not found in the materials developed to date. Using this newly developed substrate, 4 V bipolar lead/acid batteries have been built for pulsed-power applications using a special Planté formation method. The properties of this new composite substrate are investigated by using an adapted Planté formation technique. In addition, a theory is presented to describe the ratio of the specific power (P_s) and specific energy (E_s), in the case of a pulsed-power application. Using the derived P_s/E_s ratio, the bipolar lead/acid battery can be custom-designed to meet the necessary requirements.

2. Experimental

2.1. Planté formation process

Bipolar lead/acid batteries were made using the Planté method for formation of the active layers [21]. The current density was 4 mA cm^{-2} . The Planté formation method was applied in two different ways: *ex situ* (outside the battery) and *in situ* (inside the battery). For *ex situ* formation, the electrolyte composition was 10% sulfuric acid and $20 \text{ g l}^{-1} \text{ NaClO}_4 \cdot \text{H}_2\text{O}$. For *in situ* formation, the electrolyte composition was 7.4% sulfuric acid and 20 g l^{-1}

NaNO_3 . The content of sulfuric acid was lowered for *in situ* formation in order to decrease the lead sulfate formation. Nitrate was used instead of perchlorate in order to avoid the presence of residual traces of perchlorate inside the battery. 99.9% pure lead plate was used in all experiments.

2.2. Lead plating bath

For lead plating of the composite substrate, a standard fluoborate bath was used. The formulation of the bath was: $220 \text{ g l}^{-1} \text{ Pb}(\text{BF}_4)_2$, $21 \text{ g l}^{-1} \text{ HBF}_4$, $21 \text{ g l}^{-1} \text{ H}_3\text{BO}_3$ and 0.16 g l^{-1} gelatin (used as brightener). The anodes were made from lead plate (1.5 mm). The applied current density was 25 mA cm^{-2} or less. During plating, nitrogen gas was purged for bath circulation.

2.3. Preparation of lead-plated composite substrate

The composite substrate was made according to a patent pending [22]. No metals were used in order to prevent corrosion.

2.4. Properties of the composite substrate

The areal resistance was found to be equal to $0.04 \Omega \text{ cm}^2$. With a current density of 2.5 A cm^{-2} , the ohmic drop was 0.1 V.

The density of the substrate was 1.6 g cm^{-3} . The specific resistance was $1.2 \Omega \text{ cm}$. The catalytic activity towards hydrogen and oxygen evolution was found to be comparable with lead and lead dioxide. At 1 mA cm^{-2} , the overvoltage was lowered by only 10 mV, both for hydrogen and oxygen, i.e., there was a very low catalytic effect of the composite substrate.

2.5. Construction of 4 V batteries

The 4 V bipolar batteries were constructed using two lead foil (1 mm) end-plates and a lead-plated composite substrate. The thickness of the lead layer on the composite substrate was much smaller than the thickness of the lead end-plates and, therefore, determined the capacity of the battery.

The dimensions of the plates were $10 \text{ cm} \times 10 \text{ cm}$. The recombinant separator was made of glass fibre (Lydall-Ax Ω hm), thickness: 1.17 mm. This separator was compressed to 1.00 mm inside the battery in order to support the active material. The separator was placed in the same plane as the spacer (width: 1 cm and thickness: 1.00 mm). In order to avoid short circuiting, a very thin layer of insulating tape (thickness: $100 \mu\text{m}$ or less, width: 1.2 cm) was put below the spacer and separator (overlapping the region below spacer and separator). By varying the thickness of this insulating tape, the spacer distance could be varied.

To prevent heating of the battery at high current densities, a heat sink (1 K/W) was placed on either side. To lower the battery resistance, terminal plates of copper (0.2 mm thickness) were pressed on the lead end-plates. In order to prevent copper corrosion, an extra lead foil was added for protection since the lead end-plates will become porous by the Planté process.

Proper sealing was obtained using poly(methacrylate) (mixing methacrylate with 5% dibenzoylperoxide).

2.6. Planté formation

Planté formation of cells and 4 V bipolar batteries, using a lead-plated composite substrate as a bipolar plate and two lead end-plates, was performed in a two-step process: (i) one side of both cells was activated (formation of a porous lead dioxide layer) while at the other side hydrogen gas was evolved at a smooth lead surface, and (ii) the current direction was reversed resulting in the formation of the lead plates to lead dioxide and the reduction of the porous lead dioxide (formed in the first step) to porous lead. Both in situ (after construction of battery) and ex situ Planté formation (battery construction after formation) were carried out. After the Planté formation process, the bipolar battery was cycled for some tens of cycles to improve further the capacity.

2.7. Testing of 4 V bipolar batteries

The 4 V bipolar batteries with composite substrate were tested using galvanostatic charge/discharge pulses of 70 ms. Each pulse was followed by a period of 30 ms at open circuit.

In order to investigate the behaviour at different discharge rates, the discharge current density i_d (A cm^{-2}) was varied over a large range. For each value of i_d , the charge density q (C cm^{-2}) was determined. Discharging of the 4 V batteries was stopped at a battery voltage of 2 V to prevent reversal of cell voltage. Charging was performed at a current density of 50 mA cm^{-2} until there was no further increase in battery voltage.

All experiments were performed at room temperature (20°C) using 37% sulfuric acid.

3. Theory

3.1. Calculation of the Ragone plot

The calculation of the specific power P_s (in W kg^{-1}) and specific energy E_s (in Wh kg^{-1}), for obtaining the Ragone diagram, can be performed by measuring the charge density q (C cm^{-2}) as a function of the discharge current density i_d (A cm^{-2}). The value of q follows from the number of discharge pulses n_p , the discharge current

I_d (A), the discharge time t_d (s), and the plate area A (cm^2)

$$q = \frac{n_p I_d t_d}{A} \quad (1)$$

Because of the decreasing discharge voltage, a numerical averaging method was applied to determine the discharge voltage V_d .

By virtue of the presence of other components that increase the total mass of the battery (e.g., terminals, heat sinks, sealing and spacer material), it was decided to define a 2 V cell with only the following parts present: separator (including electrolyte), positive and negative active materials and composite substrate. The presence of the remaining components will, of course, decrease the values of the specific power and specific energy in a practical battery.

For the design of the battery, it is essential to know the ratio P_s/E_s . In the case of pulsed-power applications, the required ratio P_s/E_s is much higher than for electric-vehicle applications ($P_s/E_s = 5\text{--}10$), as will be shown in the model calculation below.

3.2. Model calculation of P/E ratio for pulsed-power applications

In general, power supplies that can deliver high power energy pulses repetitively consist of two main components: (i) an energy source/storage system, and (ii) an inductor. A primary energy source that is capable of delivering the desired energy for the required number of pulses but usually not at the required power level. For this, a pulse-forming network (PFN) is used and converts low power energy pulses of the source into high power energy pulses to the load (energy is conserved but the pulse width is considerably decreased by energy-compression techniques). Components of PFNs are inductors, capacitors, special rotating machines, and switch systems.

In this section, the combination of a battery (as an energy source/storage system) and an inductor (pulse transformer) as an intermediate energy storage and pulse-forming component is discussed. Fig. 1 shows the electric circuit of this combination. This application, requires a battery with high current capability and energy extraction times of tens of milliseconds. As soon as switch S is

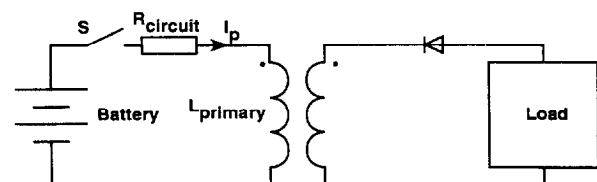


Fig. 1. Electric circuit of a battery-pulsed, transformer-based, pulsed-power supply.

closed a current will start to flow in the primary circuit (battery, R_{circuit} and L_{primary}). This current can be described as a function of time t

$$I_p(t) = I_{p(\max)} \left[1 - \exp\left(-\frac{t}{\tau}\right) \right] = \frac{V_b}{R_c} [1 - \exp(-n)] \quad (2)$$

where, $I_{p(\max)}$ is the maximum attainable current ($I_{p(\max)} = V_{\text{battery}}/R_{\text{circuit}}$) in the primary circuit and τ is the characteristic time constant of the circuit ($\tau = L_{\text{primary}}/R_{\text{circuit}}$), R_{circuit} is the total resistance in the primary circuit, and n is the normalized charging time $n = t/\tau$. As the rate of current rise is positive, the diode in the secondary is reversed biased; therefore, no secondary current flows. As soon as the primary current reaches the desired level, the switch is opened quickly and all magnetic energy stored in the primary will commutate to the secondary and result in transformation of the primary current, multiplied by the turns ratio, into the secondary circuit.

Table 1.

The energy delivered by the battery $E_b(t)$ as a function of (dis)charge time t and normalized charging time $n = t/\tau$ is given by

$$E_b = \int_0^t V_b I_p(t) dt = L_p I_{p(\max)}^2 [n - 1 + \exp(-n)] \quad (3)$$

The accumulated magnetic energy in the inductor (the primary windings of the pulse transformer) $E_L(t)$ is directly related to the current through the inductor

$$E_L(t) = \frac{1}{2} L_p I_p^2(t) = \frac{1}{2} L_p I_{p(\max)}^2 \times [1 + \exp(-2n) - 2\exp(-n)] \quad (4)$$

At the start of the charging process, all energy will be stored initially in the inductor. As the charging process progresses, more energy will increasingly be dissipated in the resistor. Therefore, the charging efficiency (η) is 100% only at the start and decreases thereafter. The longer the charging process continues, the more energy is stored in the inductor but also the more energy is dissipated in the circuit resistance. This results in a decrease in efficiency with charging time.

The charging efficiency η is given by the ratio of the

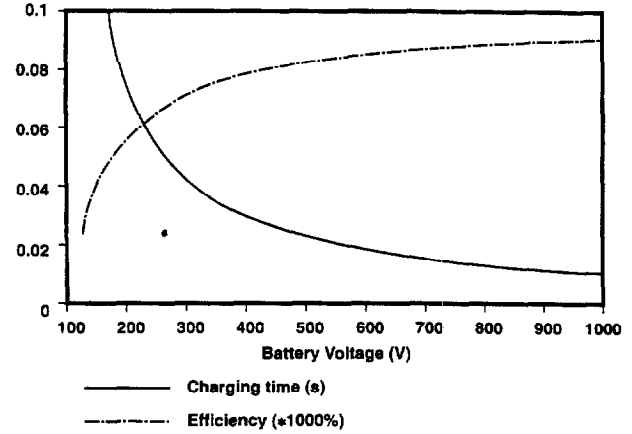


Fig. 2. Charging efficiency and time required to charge the inductor ($I_p = 10$ kA) as a function of the battery voltage: (—) charging time (s), and (---) efficiency ($\times 1000\%$).

stored magnetic energy $E_L(t)$ and the delivered battery energy $E_b(t)$

$$\eta = \frac{E_L(t)}{E_b(t)} = \frac{1 + \exp(-2n) - 2\exp(-n)}{2[n - 1 + \exp(-n)]} \quad (5)$$

For the battery/inductor combination, an optimum is desired for which: (i) the inductor is charged with the rated energy (50 kJ) at a high efficiency, and (ii) the mass of the system is as low as possible. For example, decreasing the internal resistance of the inductor decreases the dissipative losses and increases the efficiency, but at the same time increases the mass of the inductor. In this analysis, the battery only is considered and an attempt is made to optimize it for the given task/requirements, i.e., finding the desired battery voltage and size (Ah).

The following assumptions are made: the average discharge voltage per cell is 1.5 V and the areal resistance of the cell is $0.05 \Omega \text{ cm}^2$ at $i_d = 0.5 \text{ A cm}^{-2}$.

The maximum discharge current density that can be reached depends strongly on the type of lead/acid battery (thin-film, mono- or bipolar).

Fig. 2 shows, for increasing battery voltage, a decrease in charging time and an increase in charging efficiency. In order to charge the inductor up to 10 kA in 70 ms or less, a minimum battery terminal voltage of 215 V is required.

The maximum battery power P_m is $215 \text{ V} \times 10 \text{ kA} = 2.15 \text{ MW}$. The energy E delivered ($n_p \times 50 \text{ kJ}$)/ η is $34.48 \text{ MJ} = 9878 \text{ Wh}$. This results in a P/E ratio of 230 W/Wh. Comparing this source requirement with a P/E ratio of 10 W/Wh for traction batteries, indicates that a special high-power battery is being developed. If the Ragone diagram for this battery is known then the required mass of the battery can be calculated and the appropriate battery voltage and energy content chosen to optimize the battery/inductor combination. An example of a Ragone diagram is given in Fig. 3. In this diagram, the P/E figure of 230 W/Wh is also drawn. The point of intersection

Table 1
Electric circuit parameters and battery requirements

Inductance	$L = 1 \text{ mH}$
Circuit resistance without battery	$R = 10 \text{ m}\Omega$
Maximum current	$I = 10 \text{ kA}$
Stored energy	$E = 50 \text{ kJ}$
Maximum charge time inductor	$t = 70 \text{ ms}$
Number of discharges (at 10 Hz repetition rate)	$n_p = 400$

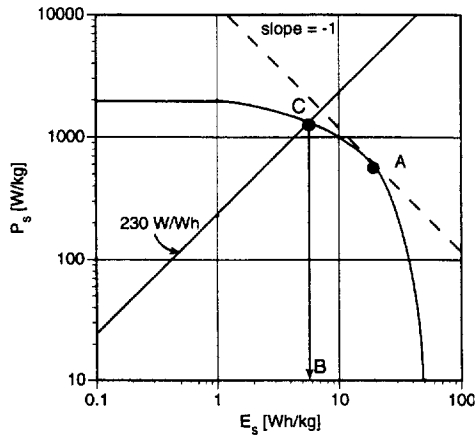


Fig. 3. Ragone diagram for a bipolar lead/acid battery.

(point C) of this line with the Ragone diagram gives point B on the specific energy axis; this point is called $E_s(B)$. The mass of the battery can now be calculated with the formula

$$M_{\text{bat}} = \frac{E_{\text{bat}}(V_b, \eta)}{E_s(B)} \quad (6)$$

E_{bat} is the energy delivered by the battery and is a function of the battery terminal voltage and charging efficiency. Increasing the battery voltage, decreases the charging time and increases the charging efficiency (see also Fig. 2), but does this also decrease the mass of the battery?

Before trying to answer this question, point A of the Ragone diagram is examined. This point is determined by $dP_s/dE_s = -1$; the product $P_s \times E_s$ has its maximum here. If the intersection of the P/E line and the Ragone diagram lies considerably to the right of point A (where the specific power rises relatively quicker than the specific energy decreases), the battery voltage should be increased and the mass of the battery will decrease. Unfortunately, in practice the point of intersection of the P/E line lies far left of point A and, therefore, increasing the voltage will not decrease the mass of the battery. A more precise optimization can only be made if the Ragone diagram of the actual battery is measured.

4. Results

4.1. Ex situ Planté formation

Ex situ Planté formation was studied using a 1 mm lead foil. The influence of the formation time on the charge density q (C cm^{-2}) is shown in Fig. 4 as a function of the discharge current density i_d .

To prevent the active material from shedding, the lead foil was pressed between several layers of glass-fibre separator. The spacing between the lead foils was 10 mm.

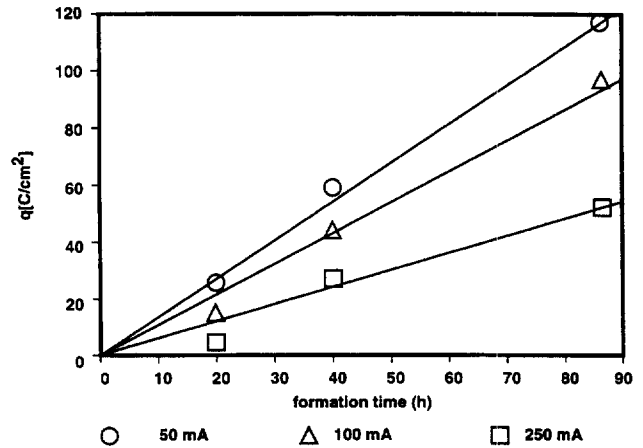
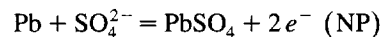
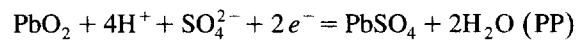


Fig. 4. Charge density q (C cm^{-2}) vs. formation time (h) for 1 mm lead foil; Planté-formation current density was 4 mA cm^{-2} : (○) 50 mA; (△) 100 mA, and (□) 250 mA.

In Fig. 4, an increase in charge density is found at longer formation time periods. This increase is found to be linear with time for different discharge current densities, see Fig. 5.

In Fig. 4, the charge density shows a strong decrease at higher discharge current densities. This behaviour, which is also found for porous plates, is caused by the limitation of the diffusion process. At the plates, the rate of the diffusion in the pores determines the rate at which active material can be used. On discharge, the following reactions occur at the positive plate (PP) and negative plate (NP), respectively



At high-discharge current densities, the pores in the PP can even become alkaline. The utilisation grade using ex

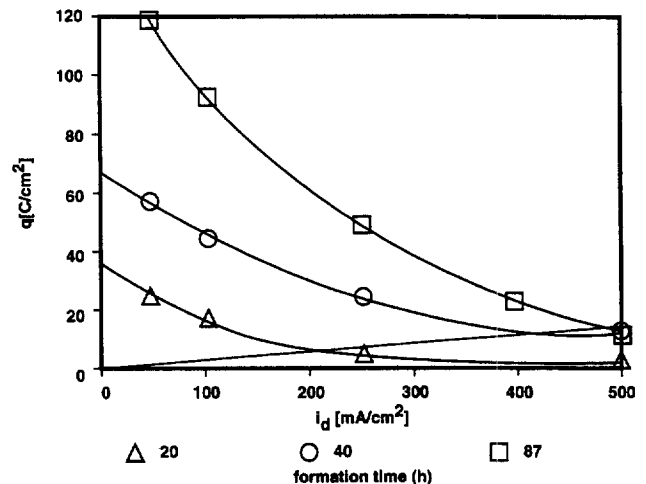


Fig. 5. Charge density q (C cm^{-2}) vs. discharge current density i_d (mA cm^{-2}) for different formation times: (△) 20 h; (○) 40 h, and (□) 87 h.

situ formation of lead foil can be calculated using Faraday's law.

In case of a lead foil of thickness d (cm), the theoretical charge density q^l (C cm^{-2}) is given by

$$q^l = \frac{dgnF}{2At} \quad (7)$$

where g is the specific weight (g cm^{-3}), $n=2$ the number of electrons, F the Faraday number, and At the atomic weight of lead.

For a lead foil of 1 mm, the value of $q^l = 528 \text{ C cm}^{-2}$ (for both sides). From Fig. 4, at $i_d = 50 \text{ mA cm}^{-2}$, a charge density of 120 C cm^{-2} is found. In this case, the utilisation grade u (%) is equal to 23%. Further lowering i_d will increase the value of u .

A straight line, starting from the origin, is drawn in Fig. 5. This line represents the charge density, as a function of i_d , for the pulsed-power application, i.e. 400 pulses of 70 ms with 30 ms rest period in between. In case of $i_d = 500 \text{ mA cm}^{-2}$, the charge density for this application equals $400 \times 0.07 \times 0.5 = 14 \text{ C cm}^{-2}$.

It must be emphasized that the pulses used in the experiments were square pulses (representing a resistive load), while for the pulsed-power application under consideration an inductive load is used (energy storage in a transformer). Discharge pulses use an inductive load start at $t = 0$ with $i_d^{\text{ind}} = 0$ and show an increase according to Eq. (8)

$$i_d^{\text{ind}} = i_d^{\text{ind, max}} \left[1 - \exp\left(\frac{-t}{\tau}\right) \right] \quad (8)$$

where $t = 0.07 \text{ s}$ and $i_d^{\text{ind, max}}$ is the maximum discharge current density for an inductive load.

The number of discharge pulses, the discharge voltage and the value of the charge density will increase using an inductive instead of a resistive load. The reason for an improved discharge capacity is caused by a diminished influence of diffusion limitations as the discharge current rises more gradually using an inductive load. In this paper, however, the tests are limited to resistive load pulses.

An important aspect of the present study is to investigate whether an ex situ or in situ Planté process should be used for designing batteries with the required specifications (i.e., high specific power with $P_s/E_s = 230 \text{ W/Wh}$).

When relatively long formation times are employed (e.g., 40 h or more), the lead foil shows severe corrosion that results in a significant increase in thickness. At 87 h, the thickness of the 1 mm lead foil becomes approximately 3–4 mm of porous material. A problem that arises is that the thickness of the active material is not uniform.

Bipolar batteries were constructed in order to test the possibility of ex situ Planté formation as a method for the preparation of the active material. To do this, $500 \mu\text{m}$ lead foil was used first (Planté formation during 8 h). Afterwards, the positive plates were reduced in 37% sulfuric acid. When constructing a 12 V bipolar battery, only

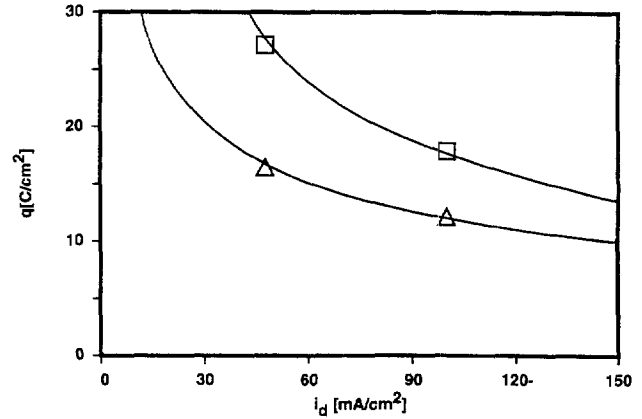


Fig. 6. Estimated course of charge density q (C cm^{-2}) vs. discharge current density i_d (mA cm^{-2}) for separate cells of 4 V bipolar lead/acid battery with composite substrate. For the active layers 1 mm lead foil was used (ex situ Planté-formed, 30 h).

Planté-formed lead foil was used. It turned out that after charging the battery to 14.4 V, the battery suffered a short circuit after two days at open circuit. After this, the battery could not be charged anymore. Unmistakenly, this can only be explained by short circuit of the electrolyte through pin holes in the corroded bipolar lead plates. This observation has an important consequence. Lead foil, activated by the Planté method, cannot be used safely as a bipolar plate. Therefore, it was necessary to develop a non-corrosive composite substrate (no metals used). Using this composite substrate, with approximately $60 \mu\text{m}$ lead coating, a 4 V bipolar battery was constructed with ex situ Planté-formed (30 h) lead foils (1 mm) for both the end plates (monopolar) and the bipolar plate. The charge density is given in Fig. 6 for both cells as a function of the discharge current density.

The large difference in capacity of both cells (each plate was tested separately as a monopolar plate and showed similar capacity) can only be explained by the non-uniform thickness of the active layer that resulted in both poor and too weak compression of the active layer by the glass-fibre separator. Which deviation in thickness of the active layer can be allowed when using the glass-fibre separator with appropriate compression? To answer this question, it is assumed that a standard glass-fibre separator of 1.17 mm is used. For high current densities, a high compression of approximately 30% is believed to give optimal results. If it is assumed that a compression between 10 and 30% is allowed, the thickness of the separator d_s lies between 0.82 and 1.05 mm. Thus, the limits of thickness of an active layer of 2.5 mm thickness are 2.385 and 2.615 mm, i.e., a maximum deviation of 5% in thickness. After 30 h of ex situ Planté formation, the thickness of the active layer varied between 2 and 3 mm. This caused the above mentioned large variation in the capacity of the separate cells. Therefore, it is concluded that ex situ formed active layers can only be used if a very narrow window for the

variation of the thickness can be accomplished. This condition is difficult to achieve, however, with relatively thick active layers (2–3 mm thickness).

4.2. In situ Planté formation

One way to solve the thickness variation of the active layer is to apply the Planté process inside the battery (in situ formation). In situ formation enables very thin layers of lead (e.g., 100 μm) to be Planté-formed (free-standing films of this thickness cannot be corroded for a long period of time because of mechanical weakness).

Since perchlorate is not wanted inside the cell, because of residual chloride after formation, nitrate (20 g l^{-1} NaNO_3) was used. The concentration of sulfuric acid was lowered from 10% (ex situ formation) to 7.4% in order to decrease the amount of lead sulfate formed. Ex situ formation showed that the use of nitrate gave stronger corrosion of the lead than perchlorate.

Using lead plated (100 μm) composite substrate (bipolar plate) and lead foil (1 mm) for the monopolar plates, a glass-fibre separator of 1.17 mm and polytetrafluoroethylene (PTFE) isolation tape, two 4 V bipolar batteries were constructed and were in situ Planté-formed for 15 and 24 h. The charge density of both batteries versus the discharge current density is given in Fig. 7.

On comparing the increase in charge density on going from 15 to 24 h formation (factor 2.5 at $i_d = 250 \text{ mA cm}^{-2}$) with data given in Fig. 5 (factor 1.5 at the same current density), it is concluded that in situ formation increases the utilization grade. This can be explained by the increased pressure on the active material at 24 h of formation due to the thickening of the lead layer. At higher compression, a better utilization of the active layer can be expected. The charge density of the lead layer (100 μm), calculated from Faraday's law, equals 105.6 C cm^{-2} at 100% utilization. For 24 h of in situ formation, at $i_d = 50 \text{ mA cm}^{-2}$, a value of 11.5 C cm^{-2} was found which corresponds with a utilization grade of 11%. This value is

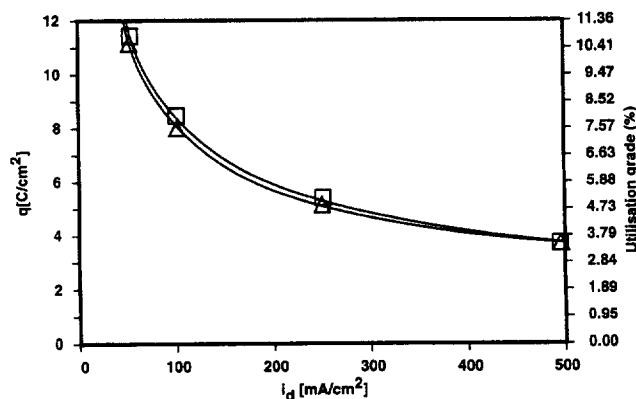


Fig. 7. Charge density q (C cm^{-2}) vs. discharge current density i_d (mA cm^{-2}) for two duplicate 4 V bipolar lead/acid batteries. Formation was in situ (24 h) using a lead-plated composite substrate.

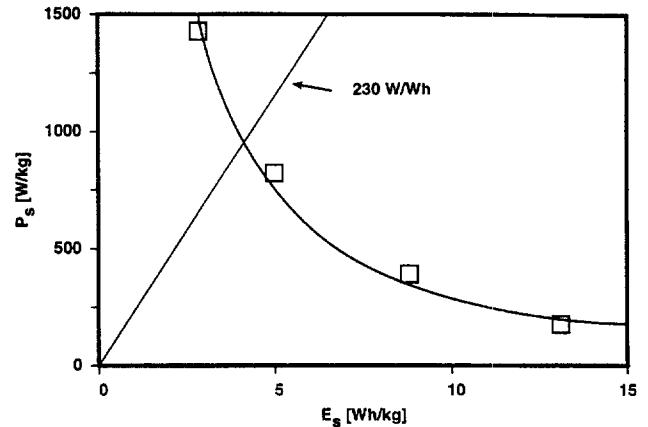


Fig. 8. Ragone plot for 24 h in situ Planté-formed 4 V bipolar lead/acid battery using lead-plated (100 μm lead composite substrate. Straight line corresponds to 230 W/Wh.

one order higher than found by Nilsson and Peterson [23] and can be explained by the higher pressure on the active material in the present case and the longer time of Planté formation.

In the manufacturing process of bipolar batteries, it is essential that the cells can be produced reproducibly. Therefore, two 4 V bipolar cells were constructed with lead-plated composite substrates that were formed in situ for 24 h (total formation time of battery was 48 h). From the similarity of both curves in Fig. 7, it is concluded that batteries made by in situ formation are highly reproducible where as ex situ formation displays very poor reproducibility.

The charge density, q , for discharge, shown in Fig. 7, was reached after 30 cycles using a discharge current density of 50 mA cm^{-2} . Discharging was terminated when the cell voltage reached 2 V. During cycling, the value of q was more than doubled.

4.3. Ragone plot

The Ragone plot was calculated for the 4 V batteries using a square centimeter of one cell. For calculating the Ragone plot, only the weight of the glass-fibre separator (thickness: 1 mm, containing 37% sulfuric acid) and the weight of the lead-plated composite substrate were taken into account. For the discharge voltage a numerical average was taken. In Fig. 8, the Ragone plot of the 4 V bipolar batteries (24 h in situ formation) is presented, together with the ratio $P_s/E_s = 230$. From the crossing of both curves, the specific power is 950 W kg^{-1} at 4.1 Wh kg^{-1} .

Compared with the values of specific power reached with thin-film monopolar lead/acid batteries (2 kW kg^{-1} and 40 Wh kg^{-1} at a discharge current density of 50 mA cm^{-2}) by Bolder Technologies, a significant improvement is necessary (see Table 2). Such an improvement is obtained by: (i) increasing the utilization grade of the lead layer by using longer formation times; (ii) lowering the

Table 2

Values for the specific power and specific energy for some recently developed lead/acid batteries (bipolar, semi-bipolar, thin-film monopolar and monopolar using gelled electrolyte)

Parameter	Bipolar	Bolder	ARA	Electrosource	JC	Panasonic	TNO	GNB
Wh kg ⁻¹	14	40	50	52	50	5	4	39
W kg ⁻¹	3500	2000	950	300	510	1600	950	300
P_s/E_s	250	50	19	6	10	320	230	8
Energy source	bipolar	monopolar	bipolar	quasi bipolar	bipolar	capacitor	bipolar	monopolar

thickness of the composite substrate; (iii) lowering the thickness of the separator from 1000 μm to, for example, 100 μm ; (iv) using another way of discharging, e.g., using an inductive load, and (v) using a thicker layer of lead (more energy) after optimizing the thickness of the composite substrate and separator.

In Table 2 [24,25], large differences exist in the ratio of P_s/E_s that depend on the type of construction and the design of the battery. True bipolar constructions are used by Bipolar Technologies, Arias Research Associates (ARA), Johnson Controls (JC) and TNO (this work). It is no surprise that only true bipolar constructions and the ultracapacitor lie within the required range of the P_s/E_s ratio.

The requirements for the pulsed-power battery (in our case) are the following: as high value as possible for P_s under the condition of $P_s/E_s = 230 \text{ W/Wh}$ and capable of a repetitive number of pulsed discharge currents of several hundreds of kA at a voltage of several hundreds of V.

The bipolar lead/acid battery preciously developed by TNO PML-Pulse Physics Laboratory [10–13] using electrochemically activated (by charging/discharging) bipolar lead plates of 1.5 mm thickness, had a specific power and energy of 1300 W kg⁻¹ and 0.013 Wh kg⁻¹ at a discharge current density of 3.4 A cm⁻². These specifications were calculated using the same method as used for the Ragone plot of Fig. 8, i.e., by taking 1 cm² of a cell and 1 mm of separator. The ratio of P_s/E_s is 10⁵, which is much higher than that required, namely, 230 W/Wh. This means that the specific energy is much too low for this application.

A semi-bipolar construction is used by Electrosource (two monopolar plates connected in one plane [26,27]). Panasonic data are for a ultracapacitor (in production) using an organic electrolyte. The data for GNB are for a conventional, sealed, recombinant battery (monopolar). The data for Bolder Technologies refer to an advanced thin-film monopolar battery.

The ultracapacitor specifications differ from batteries mostly by its relatively poor specific energy and, therefore, can only be used for high-power applications during short periods (relatively low energy is required).

It must be emphasized that the specific energy is not always shown at the given level of the specific power, but at a much lower discharge rate, e.g. $C_3/3$. The value of the specific power can be very high only if a very short discharge pulse is applied. Battery manufacturers, for ex-

ample, test specific power levels at 10 s of discharge, whereas specific energy is often based on the $C_3/3$ discharge rate. For the tests at TNO, the value of the specific energy was determined at the given specific power level during the whole discharge.

Most important for the construction of the bipolar lead/acid battery remains the required ratio P_s/E_s since this ratio determines whether a high-energy or a high-power battery is made.

Ultracapacitors that have become available recently, using thin layers of activated carbon, display a specific power of 500 W kg⁻¹ at 5 Wh kg⁻¹. With $P_s/E_s = 100$, these ultracapacitors are truly high-power energy sources with relatively low specific energy. Further improvement is predicted and it is to be expected that such ultracapacitors will become competitors with bipolar batteries in case of ratios of $P_s/E_s > 100$. Ultracapacitors will not, however, be a replacement for bipolar batteries where both relatively high specific power and energy are needed. In case of bipolar lead/acid batteries, a specific energy improvement from 40 (monopolar) to 60 Wh kg⁻¹ (bipolar) is predicted with a specific power of 200 W kg⁻¹ (monopolar) to 1000 W kg⁻¹ (bipolar). The specific energy of ultracapacitors is still less than 10 Wh kg⁻¹, which is a rather poor value compared with values for conventional lead/acid batteries.

The origin of the relatively poor specific energy for ultracapacitors lies in the absence of a faradaic process. Only the double-layer capacitance contributes to the charge stored. By using activated carbon layers, a very large specific area (500 m² g⁻¹) is obtained and results in a double-layer capacity of 150 F g⁻¹. This is equivalent to a double-layer capacitance of 30 $\mu\text{F cm}^{-2}$. The charge voltage is directed by the electrolyte composition. In case of a charge voltage of 3 V, the specific charge equals 450 C g⁻¹. A comparison with the charge that corresponds to the oxidation of 1 g of lead to lead(II) ions (using Faraday's law) yields 17000 C g⁻¹, which is a factor of 38 higher. In case of 26% utilization of the lead, the specific charge is still a factor of 10 higher. Another important disadvantage of the ultracapacitor is the linear voltage decrease during discharge.

The specific capacity of activated carbon mesobeads, developed recently [28], is 412 F g⁻¹. This value is almost a threefold increase compared with the activated carbon used in the ultracapacitor developed by Panasonic, and will

give a further impetus to the development of a next generation of ultracapacitors with increased specific energy and power.

5. Conclusions

It is shown that the bipolar lead/acid battery is an excellent candidate for battery-based, pulsed-power supplies. Although further improvement is necessary, the bipolar lead/acid battery, developed at TNO, gives promising results. At a specific power of 950 W kg^{-1} , the corresponding specific energy is 4.1 Wh kg^{-1} . These results have been obtained using a 4 V bipolar lead/acid battery prepared by an in situ Planté-formation method. For this battery, a new type of composite bipolar plate has been developed. The substrate of the bipolar plate is made of a composite material with a high conductivity and a very low catalytic activity towards hydrogen and oxygen evolution.

The employed in situ Planté formation method is a two-step process and shows great promise for further development for high-power applications.

The excellent reproducibility of the in situ formation method has been demonstrated by duplicating a 24 h formed 4 V bipolar battery using the newly developed lead-plated composite substrate. It is believed that the composite substrate can also be used in other bipolar battery systems, capacitors and fuel cells. The non-corrosive nature of the composite substrate opens the way to lightweight bipolar systems without premature failure through corrosion problems.

Acknowledgements

The authors wish to express their gratitude to D. Schmal (TNO-MEP), B. Mosterdijk and W.J. Kolkert (TNO-PML), and to B. van der Ploeg, H.E. Wijers and C. Posthumus (Royal Netherlands Navy) for their interest and stimulating discussions during the project. Further acknowledgement is given to the Royal Netherlands Navy, TNO Defence Research and TNO Environmental, Energy and Process Innovation for their financial support. The

work was carried out under Contract No. A94/KM134, A87/KM045 and A95/KM457.

References

- [1] D. Berndt and U. Teutsch, *J. Electrochem. Soc.*, 143 (1996) 790.
- [2] T. Juergens and R.F. Nelson, *J. Power Sources*, 53 (1995) 201.
- [3] D.C. Pierce, *Proc. 36th Power Sources Symp., Cherry Hill, NJ, USA, 6–9 June 1994*, p. 221.
- [4] J.L. Arias, J.J. Rowlette and E.D. Drake, *J. Power Sources*, 40 (1992) 63.
- [5] D.L. Harbaugh, *27th Int. Symp. Automotive Technology and Automation, Aachen, Germany, 1994*, p. 129.
- [6] J.J. Rowlette, *Proc. 8th Annual Battery Conf. Applications and Advances, California State University, Long Beach, CA, USA, 12–14 Jan. 1993*.
- [7] R.M. LaFollette, *Fall Meet. The Electrochemical Society, Miami Beach, FL, USA, 9–14 Oct. 1994*, p. 260.
- [8] R.M. LaFollette, *Final Rep. Ballistic Missile Defense Organization, 14 Mar. 1994*.
- [9] R.M. LaFollette, Personal communication, 23 Febr. 1995.
- [10] E. Tuinman, *7th IEEE Pulsed Power Conf., Monterey CA, USA, 1989*, pp. 134–139.
- [11] W. Karthaus, W.J. Kolkert and J. Nowee, *IEEE Trans. Magn.*, 25 (1989) 284.
- [12] N. Kaanders, W. Mosterdijk and P. Van Gelder, *9th IEEE Pulsed Power Conf., Albuquerque, NM, USA, 1993*, pp. 99–102.
- [13] A. Wollersheim and W. Mosterdijk, *TNO Rep. Eerste generatie bipolaire batterij, PML–A83, 1993*, The Netherlands.
- [14] F. Beck, G.T. Suden, U. Tormin and T. Boinowitz, *Electrochim. Acta*, 41 (1996) 933.
- [15] K. Steininger and K. Kordesch, in K. Bullock and D. Pavlov, *Proc. Symp. Advances in Lead–Acid Batteries*, Proc. Vol. 84–14, 1984, p. 406.
- [16] K.R. Bullock, *J. Power Sources*, 51 (1994) 1.
- [17] *US Patent No. 4625395* (2 Dec. 1986).
- [18] *US Patent No. 2564707* (3 Sept. 1947).
- [19] *US Patent No. 4539268* (3 Sept. 1985).
- [20] *US Patent No. 5334464* (2 Aug. 1994).
- [21] H. Bode, *Lead–Acid Batteries*, Wiley, New York, 1977.
- [22] *Dutch Patent Pend.*, (13 June 1996).
- [23] O. Nilsson and I. Peterson, *Power Sources* 15, 1995, p. 183.
- [24] A. Himy, *Final Rep. Status and Evaluation of Hybrid Electric Vehicle Batteries for Short Term Applications*, 26 July 1995, Westinghouse Electric Corporation Pittsburgh, PA.
- [25] *Kahlil*, Assorted Technical Material Battery for Combat Vehicle Working Group, 30 Aug. 1995, USA.
- [26] C.E. Hopkins, *The Battery Man*, (Sept.) (1994) 1–3.
- [27] Anon., *Advanced Battery Technology*, (Sept.) (1995) 11.
- [28] H. Shi, *Electrochim. Acta*, 41 (1996) 1633.